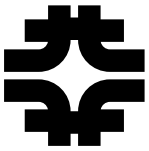

Fermi National Accelerator Laboratory

FERMILAB-Pub-99/229-E

Observation of Diffractive Beauty Production at the Fermilab Tevatron

T. Affolder et al.
The CDF Collaboration

Fermi National Accelerator Laboratory
P.O. Box 500, Batavia, Illinois 60510

August 1999

Submitted to *Physical Review Letters*

Operated by Universities Research Association Inc. under Contract No. DE-AC02-76CH03000 with the United States Department of Energy

Observation of Diffractive Beauty Production at the Fermilab Tevatron

T. Affolder,[21] H. Akimoto,[42] A. Akopian,[35] M. G. Albrow,[10] P. Amaral,[7] S. R. Amendolia,[31] D. Amidei,[24] J. Antos,[1] G. Apollinari,[35] T. Arisawa,[42] T. Asakawa,[40] W. Ashmanskas,[7] M. Atac,[10] P. Azzi-Bacchetta,[29] N. Bacchetta,[29] M. W. Bailey,[26] S. Bailey,[14] P. de Barbaro,[34] A. Barbaro-Galtieri,[21] V. E. Barnes,[33] B. A. Barnett,[17] M. Barone,[12] G. Bauer,[22] F. Bedeschi,[31] S. Belforte,[39] G. Bellettini,[31] J. Bellinger,[43] D. Benjamin,[9] J. Bensinger,[4] A. Beretvas,[10] J. P. Berge,[10] J. Berryhill,[7] S. Bertolucci,[12] B. Bevensee,[30] A. Bhatti,[35] C. Bigongiari,[31] M. Binkley,[10] D. Bisello,[29] R. E. Blair,[2] C. Blocker,[4] K. Bloom,[24] B. Blumenfeld,[17] B. S. Blusk,[34] A. Bocci,[31] A. Bodek,[34] W. Bokhari,[30] G. Bolla,[33] Y. Bonushkin,[5] K. Borras,[35] D. Bortoletto,[33] J. Boudreau,[32] A. Brandl,[26] S. van den Brink,[17] C. Bromberg,[25] N. Bruner,[26] E. Buckley-Geer,[10] J. Budagov,[8] H. S. Budd,[34] K. Burkett,[14] G. Busetto,[29] A. Byon-Wagner,[10] K. L. Byrum,[2] M. Campbell,[24] A. Caner,[31] W. Carithers,[21] J. Carlson,[24] D. Carlsmith,[43] J. Cassada,[34] A. Castro,[29] D. Cauz,[39] A. Cerri,[31] P. S. Chang,[1] P. T. Chang,[1] J. Chapman,[24] C. Chen,[30] Y. C. Chen,[1] M. -T. Cheng,[1] M. Chertok,[37] G. Chiarelli,[31] I. Chirikov-Zorin,[8] G. Chlachidze,[8] F. Chlebana,[10] L. Christofek,[16] M. L. Chu,[1] S. Cihangir,[10] C. I. Ciobanu,[27] A. G. Clark,[13] M. Cobal,[31] E. Cocca,[31] A. Connolly,[21] J. Conway,[36] J. Cooper,[10] M. Cordelli,[12] J. Guimaraes da Costa,[24] D. Costanzo,[31] J. Cranshaw,[38] D. Cronin-Hennessy,[9] R. Cropp,[23] R. Culbertson,[7] D. Dagenhart,[41] F. DeJongh,[10] S. Dell'Agnello,[12] M. Dell'Orso,[31] R. Demina,[10] L. Demortier,[35] M. Deninno,[3] P. F. Derwent,[10] T. Devlin,[36] J. R. Dittmann,[10] S. Donati,[31] J. Done,[37] T. Dorigo,[14] N. Eddy,[16] K. Einsweiler,[21] J. E. Elias,[10] E. Engels, Jr.,[32] W. Erdmann,[10] D. Errede,[16] S. Errede,[16] Q. Fan,[34] R. G. Feild,[44] C. Ferretti,[31] I. Fiori,[3] B. Flaugher,[10] G. W. Foster,[10] M. Franklin,[14] J. Freeman,[10] J. Friedman,[22] Y. Fukui,[20] S. Gadomski,[23] S. Galeotti,[31] M. Gallinaro,[35] T. Gao,[30] M. Garcia-Sciveres,[21] A. F. Garfinkel,[33] P. Gatti,[29] C. Gay,[44] S. Geer,[10] D. W. Gerdes,[24] P. Giannetti,[31] V. Glagolev,[8] M. Gold,[26] J. Goldstein,[10]

A. Gordon,[14] A. T. Goshaw,[9] Y. Gotra,[32] K. Goulianos,[35] H. Grassmann,[39] C. Green,[33] L. Groer,[36] C. Grosso-Pilcher,[7] M. Guenther,[33] G. Guillian,[24] R. S. Guo,[1] C. Haber,[21] E. Hafen,[22] S. R. Hahn,[10] C. Hall,[14] T. Handa,[15] R. Handler,[43] W. Hao,[38] F. Happacher,[12] K. Hara,[40] A. D. Hardman,[33] R. M. Harris,[10] F. Hartmann,[18] K. Hatakeyama,[35] J. Hauser,[5] J. Heinrich,[30] A. Heiss,[18] B. Hinrichsen,[23] K. D. Hoffman,[33] C. Holck,[30] R. Hollebeek,[30] L. Holloway,[16] R. Hughes,[27] J. Huston,[25] J. Huth,[14] H. Ikeda,[40] M. Incagli,[31] J. Incandela,[10] G. Introzzi,[31] J. Iwai,[42] Y. Iwata,[15] E. James,[24] H. Jensen,[10] M. Jones,[30] U. Joshi,[10] H. Kambara,[13] T. Kamon,[37] T. Kaneko,[40] K. Karr,[41] H. Kasha,[44] Y. Kato,[28] T. A. Keaffaber,[33] K. Kelley,[22] M. Kelly,[24] R. D. Kennedy,[10] R. Kephart,[10] D. Khazins,[9] T. Kikuchi,[40] M. Kirk,[4] B. J. Kim,[19] H. S. Kim,[23] S. H. Kim,[40] Y. K. Kim,[21] L. Kirsch,[4] S. Klimenko,[11] D. Knoblauch,[18] P. Koehn,[27] A. Köngeter,[18] K. Kondo,[42] J. Konigsberg,[11] K. Kordas,[23] A. Korytov,[11] E. Kovacs,[2] J. Kroll,[30] M. Kruse,[34] S. E. Kuhlmann,[2] K. Kurino,[15] T. Kuwabara,[40] A. T. Laasanen,[33] N. Lai,[7] S. Lami,[35] S. Lammel,[10] J. I. Lamoureux,[4] M. Lancaster,[21] G. Latino,[31] T. LeCompte,[2] A. M. Lee IV,[9] S. Leone,[31] J. D. Lewis,[10] M. Lindgren,[5] T. M. Liss,[16] J. B. Liu,[34] Y. C. Liu,[1] N. Lockyer,[30] M. Loreti,[29] D. Lucchesi,[29] P. Lukens,[10] S. Lusin,[43] J. Lys,[21] R. Madrak,[14] K. Maeshima,[10] P. Maksimovic,[14] L. Malferrari,[3] M. Mangano,[31] M. Mariotti,[29] G. Martignon,[29] A. Martin,[44] J. A. J. Matthews,[26] P. Mazzanti,[3] K. S. McFarland,[34] P. McIntyre,[37] E. McKigney,[30] M. Menguzzato,[29] A. Menzione,[31] E. Meschi,[31] C. Mesropian,[35] C. Miao,[24] T. Miao,[10] R. Miller,[25] J. S. Miller,[24] H. Minato,[40] S. Miscetti,[12] M. Mishina,[20] N. Moggi,[31] E. Moore,[26] R. Moore,[24] Y. Morita,[20] A. Mukherjee,[10] T. Muller,[18] A. Munar,[31] P. Murat,[31] S. Murgia,[25] M. Musy,[39] J. Nachtman,[5] S. Nahn,[44] H. Nakada,[40] T. Nakaya,[7] I. Nakano,[15] C. Nelson,[10] D. Neuberger,[18] C. Newman-Holmes,[10] C.-Y. P. Ngan,[22] P. Nicolaidi,[39] H. Niu,[4] L. Nodulman,[2] A. Nomerotski,[11] S. H. Oh,[9] T. Ohmoto,[15] T. Ohsugi,[15] R. Oishi,[40] T. Okusawa,[28] J. Olsen,[43] C. Pagliarone,[31] F. Palmonari,[31] R. Paoletti,[31] V. Papadimitriou,[38] S. P. Pappas,[44] A. Parri,[12] D. Partos,[4] J. Patrick,[10] G. Pauletta,[39] M. Paulini,[21] A. Perazzo,[31] L. Pescara,[29] T. J. Phillips,[9] G. Piacentino,[31] K. T. Pitts,[10] R. Plunkett,[10] A. Pompos,[33] L. Pondrom,[43] G. Pope,[32] F. Prokoshin,[8] J. Proudfoot,[2]

F. Ptohos,[12] G. Punzi,[31] K. Ragan,[23] D. Reher,[21] A. Ribon,[29] F. Rimondi,[3] L. Ristori,[31] W. J. Robertson,[9] A. Robinson,[23] T. Rodrigo,[6] S. Rolli,[41] L. Rosenson,[22] R. Roser,[10] R. Rossin,[29] W. K. Sakumoto,[34] D. Saltzberg,[5] A. Sansoni,[12] L. Santi,[39] H. Sato,[40] P. Savard,[23] P. Schlabach,[10] E. E. Schmidt,[10] M. P. Schmidt,[44] M. Schmitt,[14] L. Scodellaro,[29] A. Scott,[5] A. Scribano,[31] S. Segler,[10] S. Seidel,[26] Y. Seiya,[40] A. Semenov,[8] F. Semeria,[3] T. Shah,[22] M. D. Shapiro,[21] P. F. Shepard,[32] T. Shibayama,[40] M. Shimojima,[40] M. Shochet,[7] J. Siegrist,[21] G. Signorelli,[31] A. Sill,[38] P. Sinervo,[23] P. Singh,[16] A. J. Slaughter,[44] K. Sliwa,[41] C. Smith,[17] F. D. Snider,[10] A. Solodsky,[35] J. Spalding,[10] T. Speer,[13] P. Sphicas,[22] F. Spinella,[31] M. Spiropulu,[14] L. Spiegel,[10] L. Stanco,[29] J. Steele,[43] A. Stefanini,[31] J. Strologas,[16] F. Strumia, [13] D. Stuart,[10] K. Sumorok,[22] T. Suzuki,[40] R. Takashima,[15] K. Takikawa,[40] M. Tanaka,[40] T. Takano,[28] B. Tannenbaum,[5] W. Taylor,[23] M. Tecchio,[24] P. K. Teng,[1] K. Terashi,[40] S. Tether,[22] D. Theriot,[10] R. Thurman-Keup,[2] P. Tipton,[34] S. Tkaczyk,[10] K. Tollefson,[34] A. Tollestrup,[10] H. Toyoda,[28] W. Trischuk,[23] J. F. de Troconiz,[14] S. Truitt,[24] J. Tseng,[22] N. Turini,[31] F. Ukegawa,[40] J. Valls,[36] S. Vejcik III,[10] G. Velev,[31] R. Vidal,[10] R. Vilar,[6] I. Vologouev,[21] D. Vucinic,[22] R. G. Wagner,[2] R. L. Wagner,[10] J. Wahl,[7] N. B. Wallace,[36] A. M. Walsh,[36] C. Wang,[9] C. H. Wang,[1] M. J. Wang,[1] T. Watanabe,[40] T. Watts,[36] R. Webb,[37] H. Wenzel,[18] W. C. Wester III,[10] A. B. Wicklund,[2] E. Wicklund,[10] H. H. Williams,[30] P. Wilson,[10] B. L. Winer,[27] D. Winn,[24] S. Wolbers,[10] D. Wolinski,[24] J. Wolinski,[25] S. Worm,[26] X. Wu,[13] J. Wyss,[31] A. Yagil,[10] W. Yao,[21] G. P. Yeh,[10] P. Yeh,[1] J. Yoh,[10] C. Yosef,[25] T. Yoshida,[28] I. Yu,[19] S. Yu,[30] A. Zanetti,[39] F. Zetti,[21] and S. Zucchelli[3]

(CDF Collaboration)

[1] *Institute of Physics, Academia Sinica, Taipei, Taiwan 11529, Republic of China*

[2] *Argonne National Laboratory, Argonne, Illinois 60439*

[3] *Istituto Nazionale di Fisica Nucleare, University of Bologna, I-40127 Bologna, Italy*

[4] *Brandeis University, Waltham, Massachusetts 02254*

[5] *University of California at Los Angeles, Los Angeles, California 90024*

[6] *Instituto de Fisica de Cantabria, University of Cantabria, 39005 Santander, Spain*

[7] *Enrico Fermi Institute, University of Chicago, Chicago, Illinois 60637*

[8] *Joint Institute for Nuclear Research, RU-141980 Dubna, Russia*

[9] *Duke University, Durham, North Carolina 27708*

[10] *Fermi National Accelerator Laboratory, Batavia, Illinois 60510*

[11] *University of Florida, Gainesville, Florida 32611*

[12] *Laboratori Nazionali di Frascati, Istituto Nazionale di Fisica Nucleare, I-00044 Frascati, Italy*

[13] *University of Geneva, CH-1211 Geneva 4, Switzerland*

[14] *Harvard University, Cambridge, Massachusetts 02138*

[15] *Hiroshima University, Higashi-Hiroshima 724, Japan*

[16] *University of Illinois, Urbana, Illinois 61801*

[17] *The Johns Hopkins University, Baltimore, Maryland 21218*

[18] *Institut für Experimentelle Kernphysik, Universität Karlsruhe, 76128 Karlsruhe, Germany*

[19] *Korean Hadron Collider Laboratory: Kyungpook National University, Taegu 702-701; Seoul National University, Seoul 151-742; and SungKyunKwan University, Suwon 440-746; Korea*

[20] *High Energy Accelerator Research Organization (KEK), Tsukuba, Ibaraki 305, Japan*

[21] *Ernest Orlando Lawrence Berkeley National Laboratory, Berkeley, California 94720*

[22] *Massachusetts Institute of Technology, Cambridge, Massachusetts 02139*

[23] *Institute of Particle Physics: McGill University, Montreal H3A 2T8; and University of Toronto, Toronto M5S 1A7; Canada*

[24] *University of Michigan, Ann Arbor, Michigan 48109*

[25] *Michigan State University, East Lansing, Michigan 48824*

[26] *University of New Mexico, Albuquerque, New Mexico 87131*

[27] *The Ohio State University, Columbus, Ohio 43210*

[28] *Osaka City University, Osaka 588, Japan*

[29] *Universita di Padova, Istituto Nazionale di Fisica Nucleare, Sezione di Padova, I-35131 Padova, Italy*

[30] *University of Pennsylvania, Philadelphia, Pennsylvania 19104*

[31] *Istituto Nazionale di Fisica Nucleare, University and Scuola Normale Superiore of Pisa, I-56100 Pisa, Italy*

[32] *University of Pittsburgh, Pittsburgh, Pennsylvania 15260*

[33] *Purdue University, West Lafayette, Indiana 47907*

[34] *University of Rochester, Rochester, New York 14627*

[35] *Rockefeller University, New York, New York 10021*

[36] *Rutgers University, Piscataway, New Jersey 08855*

[37] *Texas A&M University, College Station, Texas 77843*

[38] *Texas Tech University, Lubbock, Texas 79409*

[39] *Istituto Nazionale di Fisica Nucleare, University of Trieste/ Udine, Italy*

[40] *University of Tsukuba, Tsukuba, Ibaraki 305, Japan*

[41] *Tufts University, Medford, Massachusetts 02155*

[42] *Waseda University, Tokyo 169, Japan*

[43] *University of Wisconsin, Madison, Wisconsin 53706*

[44] *Yale University, New Haven, Connecticut 06520*

Abstract

We report a measurement of the fraction of b-quarks produced diffractively in $\bar{p}p$ collisions at $\sqrt{s}$=1.8 TeV. Diffraction is identified by the absence of particles in a forward pseudorapidity region. From events with an electron of transverse momentum $9.5 < p_T^e < 20$ GeV/c within the pseudorapidity region $|\eta|$ <1.1, the ratio of diffractive to total b-quark production rates is found to be $R_{\bar{b}b} = [0.62 \pm 0.19(stat) \pm 0.16(syst)]\%$. This result is comparable in magnitude to corresponding ratios for W and dijet production, but significantly lower than expectations based on factorization.

PACS number(s): 12.40.Nn, 13.20.He

Typeset using REVTEX

We report the first observation of diffractive b-quark production. In two previous letters we reported results on diffractive W-boson [1] and dijet [2] production in $\bar{p}p$ collisions at $\sqrt{s} = 1800$ GeV at the Fermilab Tevatron. From the ratio of the W to dijet production rates, the gluon fraction of the Pomeron, which is presumed to be exchanged in diffractive processes, was measured [2] to be $f_g = (0.7 \pm 0.2)$. This result agrees with the values of f_g obtained at the HERA electron-proton collider by the ZEUS [3] and H1 [4] collaborations. However, the production rates at the Tevatron are 5-10 times lower than predictions [5,6] based on the "diffractive structure function" of the proton measured at HERA. This breakdown of factorization brings into question the proposed [7] picture of the Pomeron as a color singlet state with a hadron-like structure function.

To probe more directly the gluon component of the Pomeron, we extended our studies to diffractive $\bar{b}b$ production. The UA1 collaboration set an upper limit of 1.2 μb (0.6 μb) at 95% CL on the total diffractive b-quark production cross section in $\bar{p}p$ collisions at $\sqrt{s} = 630$ GeV, assuming a soft (hard) gluonic Pomeron structure in evaluating the detector acceptance [8]. The corresponding upper limit on the ratio of the diffractive to total [9] cross sections is $R_{\bar{b}b} =$ 6.2 (3.1) %. In this letter, we report a measurement of $R_{\bar{b}b}$ in $\bar{p}p$ collisions at $\sqrt{s} = 1800$ GeV using the Collider Detector at Fermilab (CDF). Our measurement is based on identifying a high transverse momentum electron from b-quark decay, within the pseudorapidity [10] region $|\eta| < 1.1$, produced in single diffraction dissociation, $p + \bar{p} \rightarrow p/\bar{p} + b(\rightarrow e + X') + X$. Diffractive production is tagged by the requirement of a "rapidity gap", defined as the absence of particles in a forward pseudorapidity region.

The detector is described in detail elsewhere [11,12]. In the rapidity gap analysis we use the beam-beam counters (BBC) and the forward calorimeters. The BBC consist of two arrays of eight vertical and eight horizontal scintillation counters perpendicular to the beam line at $z = \pm 5.8$ m and cover approximately the region $3.2 < |\eta| < 5.9$. The fiducial region of the forward calorimeters covers the range $2.4 < |\eta| < 4.2$ with projective towers of size $\Delta\eta \times \Delta\phi = 0.1 \times 5^\circ$. The detector components relevant to electron detection and b-quark identification in the region of $|\eta| < 1.1$ are the microstrip silicon vertex detector (SVX), the central

tracking chamber (CTC), and the central electromagnetic (CEM) and hadronic calorimeters surrounding the CTC. Proportional strip chambers at the CEM shower maximum position provide shower profile measurements, and a preshower detector, consisting of multiwire proportional chambers placed in front of the CEM, is used to help separate electrons from hadrons by sampling the showers initiated in the 1.075 radiation-length solenoid magnet coil. The transverse profile of the interacting beams at $z = 0$ is circular with r.m.s. radius of 25 μm. The SVX provides an accurate measurement of the impact parameter of tracks in the r-ϕ plane [12], and the CTC provides momentum analysis for charged particles with a resolution of $\sigma_{p_T}/p_T = 0.002(\mathrm{GeV}/c)^{-1} p_T$.

The data used in this analysis are from the 1994-95 run (80 pb^{-1}), collected with a trigger requiring an electron candidate of $E_T^e > 7.5$ GeV within $|\eta| < 1.1$. To avoid trigger theshold effects, only events with $E_T^e > 9.5$ GeV are retained. To help identify electrons and reject hadronic background [13], we consider the longitudinal and lateral shower profiles, require matching in energy and lateral position between the shower and the electron candidate track, and demand that the preshower signal be consistent with that expected for an electron. Events with electrons from W and Z bosons are rejected by requiring $E_T^e < 20$ GeV and missing transverse energy $\not\!\!E_T < 20$ GeV. The background of electrons from photon conversions in detector material between the beam line and the CTC, as well as from Dalitz pairs, is removed by rejecting events with an oppositely charged track within a small opening angle from the electron candidate. The rejection efficiency of conversion electrons is $\sim 80\%$. In addition to the electron candidate, each event is required to have a jet consisting of at least two CTC tracks. Jets are selected by a clustering algorithm using $p_T > 1$ GeV/c for the seed track and $p_T > 0.4$ GeV/c for additional tracks within a cone of radius $(\Delta\eta^2 + \Delta\phi^2)^{1/2} < 0.4$. If more than one jets are found, the one closest to the electron candidate is used. From the jet tracks we construct a jet axis which is used in the separation between bottom and charm quark decays. The above requirements are satisfied by 161,775 events. Our analysis strategy consists of first extracting a diffractive signal from this event sample and then evaluating the b-quark fraction separately in the diffractive and total event

samples.

As in our previous studies [1,2], the diffractive signal is evaluated by counting BBC hits, N_{BBC}, and adjacent forward calorimeter towers, N_{CAL}, with $E > 1.5$ GeV. Figure 1a shows the correlation between N_{BBC} and N_{CAL}. There are two entries per event in this figure, one for the positive and the other for the negative η side of the detector. The (0,0) bin, N_{BBC}=N_{CAL}=0, contains 100 events. The excess of events in this bin above a smooth extrapolation from nearby bins is attributed to diffractive production. The non-diffractive content of the (0,0) bin is evaluated from the distribution of events along the diagonal of Fig. 1a with $N_{BBC} = N_{CAL}$, shown in Fig. 1b. An extrapolation to bin (0,0) of a fit to the data of bins (2,2) to (9,9) yields 24.4 ± 5.5 non-diffractive background events. In the following, the subsample of events in the (0,0) bin will be referred to as "diffractive".

Figures 1c and 1d show the electron E_T and η distribution, respectively, for the diffractive and total event samples. In Fig. 1d, the sign of the electron pseudorapidity for events with a gap at positive η was changed. We observe that while the E_T spectra show no significant difference, the diffractive η distribution is shifted away from the gap relative to the symmetric distribution of the total event sample. The dips seen in the latter are due to losses occuring at the interfaces between different calorimeter sections and are adequately reproduced by Monte Carlo simulations.

In addition to events from b-quark decays, the data contain events from charm decays and background. The background is mainly due to hadrons faking electrons and to electrons from residual photon conversions. Using the distribution of the charge deposited in the preshower detector, the hadron background in the total [diffractive] event sample is estimated to be $(25.8 \pm 0.7)\%$ $[(30.5 \pm 5.1)\%]$. Our estimate of the residual photon conversion background is $(3.0 \pm 0.1)\%$ $[(2.1 \pm 0.7)\%]$.

The beauty and charm fractions in the data are evaluated separately for the diffractive and total event samples. We use two methods to discriminate between beauty and charm decays. In the first method, we fit the electron momentum component perpendicular to the jet axis, $p_T^{e/jet}$, which depends on the mass of the parent quark, with the sum of four tem-

plates: fake electrons from hadrons, photon conversions, charm and beauty. The amounts of fake electrons and photon conversions, for which the templates were obtained from data, are constrained by the estimates given above. The charm and beauty templates were obtained from simulations using the PYTHIA Monte Carlo generator [14], followed by a detector simulation. This 4-component fit yields a beauty fraction of $(42.9 \pm 0.4)\%$ $[(38 \pm 14)\%]$ for the total [diffractive] event sample. The second method uses the impact parameter of the electron track, which depends on both the mass and the lifetime of the parent quark. The impact parameter is defined as the minimum distance between the primary vertex and the electron track in the r-ϕ plane. A fit to the impact parameter distribution using four templates, as above, yields $(47.7 \pm 0.4)\%$ $[(38 \pm 14)\%]$ for our two data samples.

Figures 2a and 2b show the fits to the $p_T^{e/jet}$ and impact parameter distributions of the total event sample. Averaging the results of the two methods yields $73371 \pm 485(stat) \pm 7774(syst)$ beauty events, where as systematic uncertainty we assigned the difference between the results of the two methods. Figures 2c and 2d show a simultaneous fit to the $p_T^{e/jet}$ and impact parameter distributions of the diffractive sample. This fit yields $44.4 \pm 10.2(stat) \pm 4.7(syst)$ beauty events, where we assigned the same relative systematic uncertainty as that in the total event sample. After subtracting the 24% non-diffractive background estimated from the fit in Fig. 1b, there remain $33 \pm 10(stat) \pm 5(syst)$ diffractive beauty events.

The diffractive event yield must be corrected for losses caused by additional $\bar{p}p$ interactions occurring in the same $\bar{p}p$ bunch crossing as a diffractive event, as well as for BBC and forward calorimeter occupancy due to noise or beam associated backgrounds. Such occurrences would spoil the rapidity gap. From the instantaneous luminosity during data collection and the known cross section for inelastic $\bar{p}p$ collisions, the fraction of events for which a rapidity gap is not spoiled by another interaction is found to be 0.26 ± 0.01. Using a sample of events with no reconstructed primary vertex collected by triggering the detector on randomly selected beam crossings, the combined BBC and calorimeter occupancy was measured to be 0.23 ± 0.07. Correcting for these losses yields $165 \pm 50(stat) \pm 29(syst)$

diffractive beauty events.

The diffractive to total b-quark production ratio obtained from the above numbers is $R_{b\bar{b}}^{\rm gap} = [0.23 \pm 0.07(stat) \pm 0.05(syst)]\%$. This ratio is based on diffractive events satisfying our rapidity gap definition. To evaluate $R_{b\bar{b}}$ for the total diffractive beauty production requires knowledge of the rapidity gap acceptance, defined as the ratio of the number of diffractive events with a rapidity gap to the number of all diffractive events. The acceptance is calculated using the POMPYT [15] Monte Carlo generator followed by a detector simulation. In POMPYT, Pomerons emitted by the $p(\bar{p})$ interact with the $\bar{p}(p)$ in collisions simulated by PYTHIA [14]. As in our previous papers [1,2], we use the standard Pomeron flux factor of Regge theory, $f_{I\!P/p}(\xi,t) = K\xi^{1-2\alpha(t)}\, F^2(t)$, where ξ is the fraction of the beam momentum carried by the Pomeron, t is the 4-momentum transfer squared, $\alpha(t) = 1.115 + 0.26\,t$ is the Pomeron Regge trajectory, $F(t)$ the proton form factor, and $K = 0.73$ GeV^{-2} [16]. The acceptance was calculated for $\xi < 0.1$ and the same requirements for b-quark selection as for the data, using either a flat, $\beta f(\beta) = 1$, or a hard, $\beta f(\beta) = 6\beta(1-\beta)$, structure function for the Pomeron, where β is the fraction of the momentum of the Pomeron carried by a parton. The results are shown in the table below:

Rapidity gap acceptance.

$I\!P$-structure	flat-g	flat-q	hard-g	hard-q
Acceptance	0.41±0.02	0.27±0.02	0.36±0.03	0.22±0.02

The rapidity gap acceptance for events generated with a flat Pomeron structure, which is favored by the HERA measurements [3,4], and a gluon fraction of 0.7 ± 0.2, as reported in [2], is found to be 0.37 ± 0.02. Dividing $R_{b\bar{b}}^{\rm gap}$ by this value yields a diffractive to total production ratio of

$$R_{b\bar{b}} = [0.62 \pm 0.19(stat) \pm 0.16(syst)]\% \ \ (\xi < 0.1).$$

Figure 3 shows a MC generated Pomeron ξ distribution for diffractive $b \to e + X$ events with an electron of $p_T > 9.5$ GeV/c within $|\eta| < 1.1$. The shaded area represents events

with a BBC and forward calorimeter rapidity gap as defined in this analysis. The events are concentrated in the region of $0.01 < \xi < 0.06$.

Theoretical calculations based on factorization using parton densities derived from fits to HERA measurements predict values for $R_{\bar{b}b}$ ranging from 3.9% to 20.8% for the favored "high-glue" fits, depending on the type of fit used [18]. From POMPYT, using the standard Pomeron flux and a flat (hard) Pomeron structure consisting of purely gluons or quarks, we obtain 10.4% (11.6%) and 0.92% (1.02%), respectively. The ratio D of the measured $R_{\bar{b}b}$ fraction to that predicted by POMPYT depends on the gluon fraction f_g of the Pomeron. This is shown in Fig. 4, where D is plotted as a function of f_g along with published results from ZEUS and our previous measurements [1,2]. For each measurement the two curves show the 1σ bounds. Since the curves for the published results were obtained using a hard Pomeron structure in POMPYT, we used a hard structure in the b case as well. The resulting curves are almost indistinguishable from those obtained with a flat Pomeron structure. The black cross and shaded ellipse represent the best fit and 1σ contour of a least square two-parameter fit to the three CDF results. This fit had $\chi^2 = 1.7$, and therefore the ellipse was calculated after multiplying the errors in the measured diffractive to total ratios by $\sqrt{1.7}$ [17]. The fit yielded $D_{CDF} = 0.19 \pm 0.04$ and $f_g^{CDF} = 0.54^{+0.16}_{-0.14}$, in agreement with the results we obtained from the W and dijet rates, namely $D = 0.18 \pm 0.04$ and $f_g = 0.7 \pm 0.2$ [2]. The value of D_{CDF} is significantly smaller than the ZEUS result. The discrepancy between the HERA and Tevatron D-values represents a breakdown of factorization. The magnitude of the suppression of D at the Tevatron is in agreement with predictions [5] based on the renormalized Pomeron flux model [16], in which the Pomeron flux integral over all available phase space is set to unity.

In conclusion, we have made the first observation of diffractive beauty production in $\bar{p}p$ collisions at $\sqrt{s} = 1800$ GeV and measured the ratio of the diffractive to total production rates to be $R_{\bar{b}b} = [0.62 \pm 0.19(stat) \pm 0.16(syst)]\%$ $(\xi < 0.1)$ for events with an electron from $b \to e + X$ with $9.5 < p_T^e < 20$ GeV/c within $|\eta| < 1.1$. The value of $R_{\bar{b}b}$ is comparable in magnitude to the values of R_W and R_{JJ} obtained previously for W and dijet production,

but significantly lower than expectations based on factorization.

We thank the Fermilab staff and the technical staffs of the participating institutions for their vital contributions. This work was supported by the U.S. Department of Energy and National Science Foundation; the Italian Istituto Nazionale di Fisica Nucleare; the Ministry of Education, Science and Culture of Japan; the Natural Sciences and Engineering Research Council of Canada; the National Science Council of the Republic of China; the A.P.Sloan Foundation; and the Max Kade Foundation.

REFERENCES

[1] F. Abe *et al.*, Phys. Rev. Lett. **78**, 2698 (1997).

[2] F. Abe *et al.*, Phys. Rev. Lett. **79**, 2636 (1997).

[3] M. Derrick *et al.*, Z. Phys. **C 68**, 569 (1995); Phys. Lett. **B 356**, 129 (1995); Eur. Phys. J. **C 6**, 43 (1999).

[4] T. Ahmed *et al.*, Phys. Lett. **B 348**, 681 (1995); C. Adloff *et al.*, Z. Phys. **C 76**, 613 (1997).

[5] K. Goulianos, in *Proceedings of "Vth International Workshop on Deep Inelastic Scattering and QCD,"* Chicago, USA, 1997, edited by J. Repond and D. Krakauer (AIP Conf. Proc. **407**, 1997) pp. 527-532.

[6] L. Alvero, J. C. Collins, J. Terron and J. Whitmore, Phys. Rev. **D 59**, 074022 (1999).

[7] G. Ingelman and P. Schlein, Phys. Lett. **B 152**, 256 (1985).

[8] K. Wacker, in *Proceedings of "VIIth Topical Workshop on Proton-Antiproton Collider Physics,"* edited by Rajendran Raja, Alvin Tollestrup, and John Yoh (World Scientific, 1989) pp. 611-628.

[9] C. Albajar *et al.*, Phys. Lett. **B 256**, 121 (1991).

[10] We use rapidity and pseudorapidity, η, interchangeably; $\eta \equiv -\ln(\tan\frac{\theta}{2})$, where θ is the polar angle of a particle with respect to the proton beam direction. The azimuthal angle is denoted by ϕ, and transverse energy is defined as $E_T = E\sin\theta$.

[11] F. Abe *et al.*, Nucl. Instrum. Methods Phys. Res., Sect. **A 271**, 387 (1988).

[12] D. Amidei *et al.*, Nucl. Instrum. Methods Phys. Res., Sect. **A 350**, 73 (1994); P. Azzi *et al.*, Nucl. Instrum. Methods Phys. Res., Sect. **A 360**, 137 (1995).

[13] F. Abe *et al.*, Phys. Rev. **D 52**, 2624 (1995).

[14] T. Sjöstrand, Comput. Phys. Commun. **82**, 74 (1994).

[15] P. Bruni, A. Edin and G. Ingelman, http://www3.tsl.uu.se/thep/pompyt/

[16] K. Goulianos, Phys. Lett. **B 358**, 379 (1995); Phys. Lett. **B 363**, 268 (1995).

[17] R. Barnett *et al.*, Review of Particle Physics, Phys. Rev. **D** 54, 1 (1996), Sec. 4.2.2.

[18] L. Alvero, J. C. Collins and J. Whitmore, hep-ph/9806340.

FIGURES

FIG. 1. (a) Forward calorimeter tower multiplicity, N_{CAL}, versus beam-beam counter multiplicity, N_{BBC}; (b) multiplicity distribution along the diagonal with $N_{BBC} = N_{CAL}$ in the plot in (a); (c) electron E_T and (d) pseudorapidity for the diffractive (points) and total (histogram) event samples (diffractive events with a rapidity gap at positive η are entered with the sign of the electron η changed).

FIG. 2. (a) Electron transverse momentum relative to the jet, $p_T^{e/jet}$, and (b) impact parameter of the electron track for the total event sample, shown with a fit to contributions from hadrons (fake electrons), photon conversions, charm, and beauty; (c) and (d) show the same distributions for the diffractive sample (0-0 bin in Fig. 1a) with a simultaneous fit to the four components of both distributions.

FIG. 3. Monte Carlo distribution of the Pomeron beam momentum fraction, ξ, for diffractive beauty production events with an electron of $9.5 < p_T^e < 20$ GeV/c within $|\eta| < 1.1$, generated using a flat Pomeron structure of gluon to quark ratio $0.7 \div 0.3$. The shaded area is the distributions for events satisfying the rapidity gap requirements.

FIG. 4. The ratio, D, of measured to predicted diffractive rates as a function of the gluon content of the Pomeron. The predictions are from POMPYT using the standard Pomeron flux and a hard Pomeron structure. The CDF-W curves were calculated assuming a three-flavor quark structure for the Pomeron. The black cross and shaded ellipse are the best fit and 1σ contour of a least square two-parameter fit to the three CDF results.

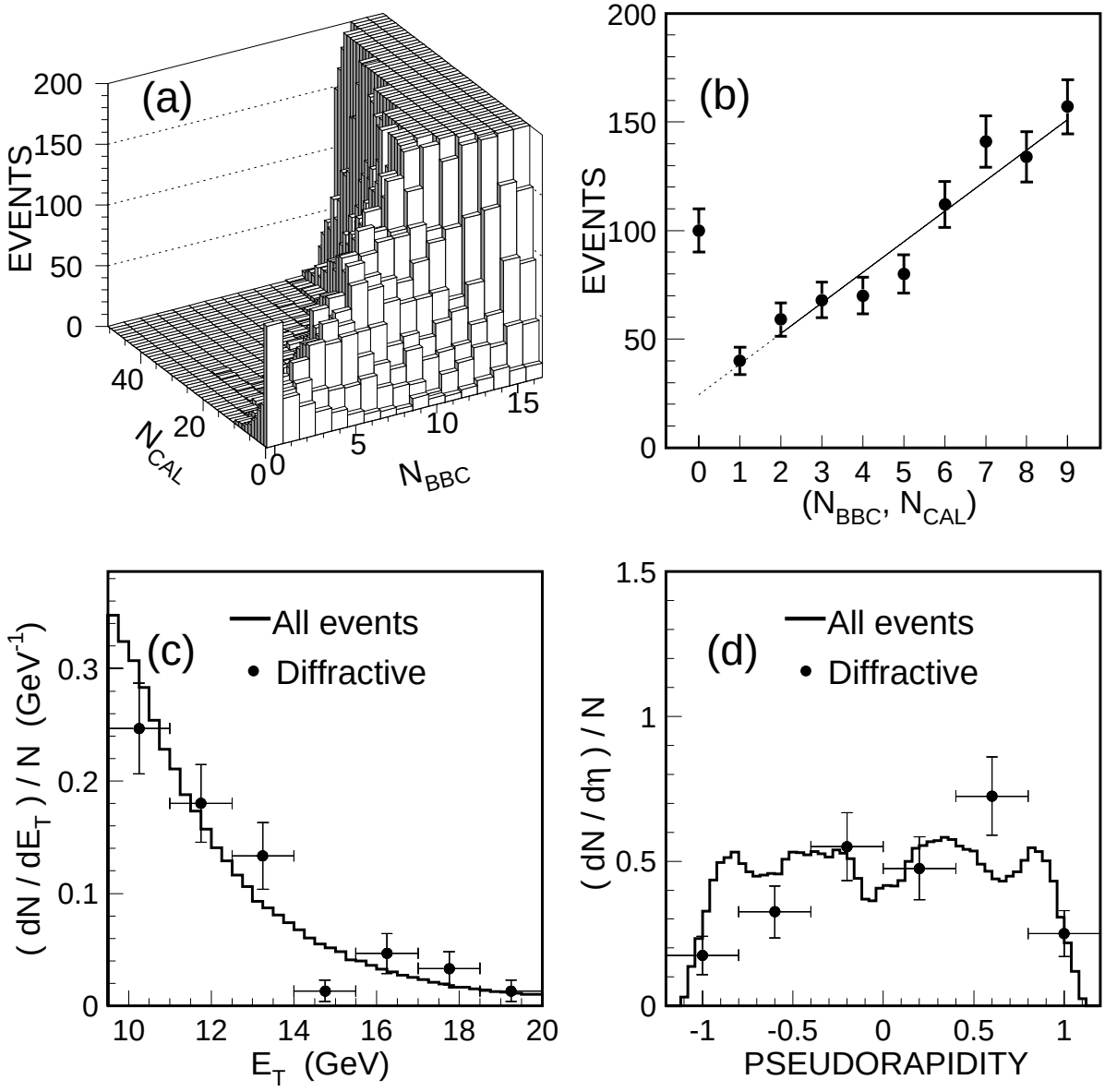

FIG. 1. (a) Forward calorimeter tower multiplicity, N_{CAL}, versus beam-beam counter multiplicity, N_{BBC}; (b) multiplicity distribution along the diagonal with $N_{BBC} = N_{CAL}$ in the plot in (a); (c) electron E_T and (d) pseudorapidity for the diffractive (points) and total (histogram) event samples (diffractive events with a rapidity gap at positive η are entered with the sign of the electron η changed).

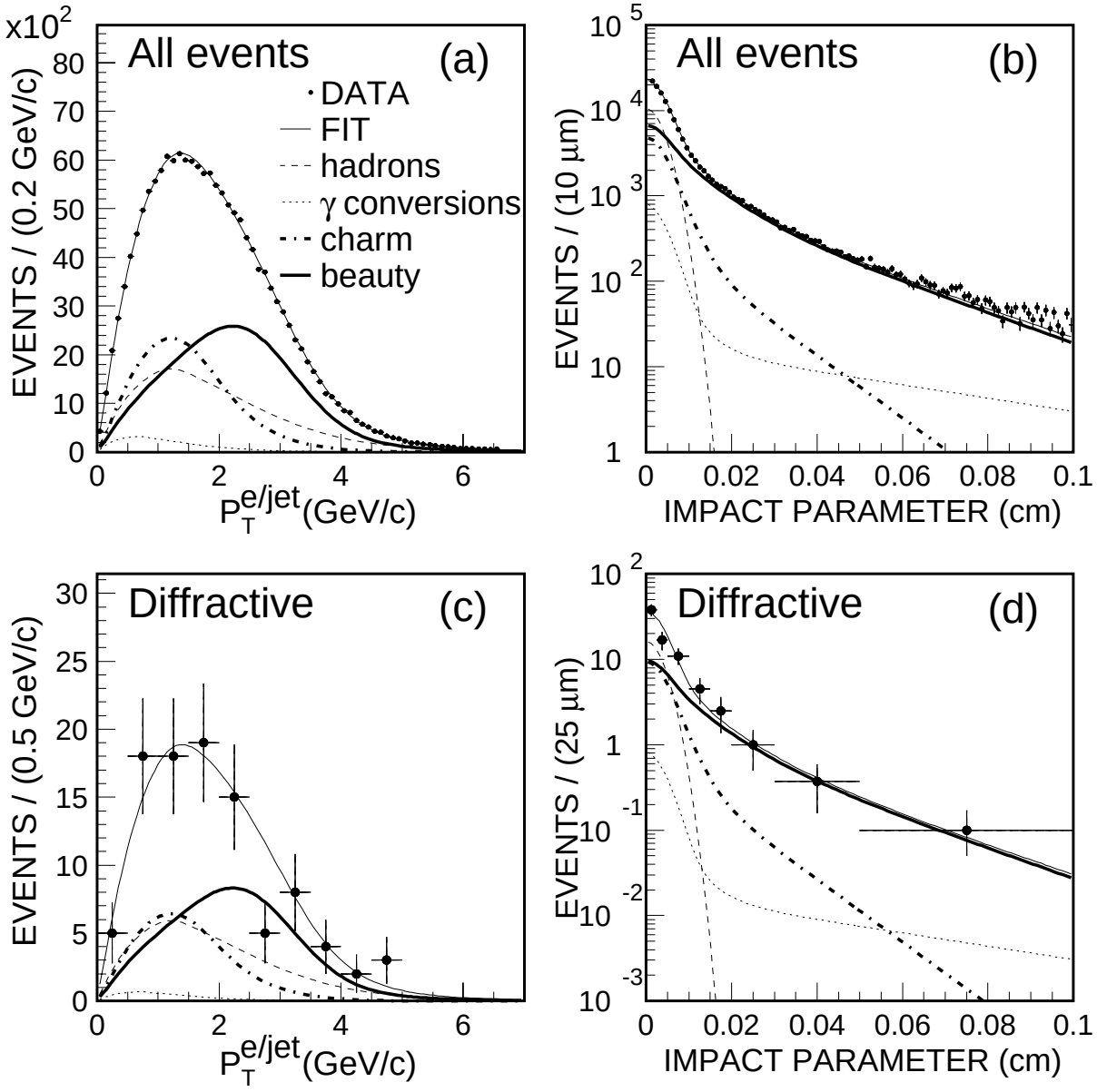

FIG. 2. (a) Electron transverse momentum relative to the jet, $p_T^{e/jet}$, and (b) impact parameter of the electron track for the total event sample, shown with a fit to contributions from hadrons (fake electrons), photon conversions, charm, and beauty; (c) and (d) show the same distributions for the diffractive sample (0-0 bin in Fig. 1a) with a simultaneous fit to the four components of both distributions.

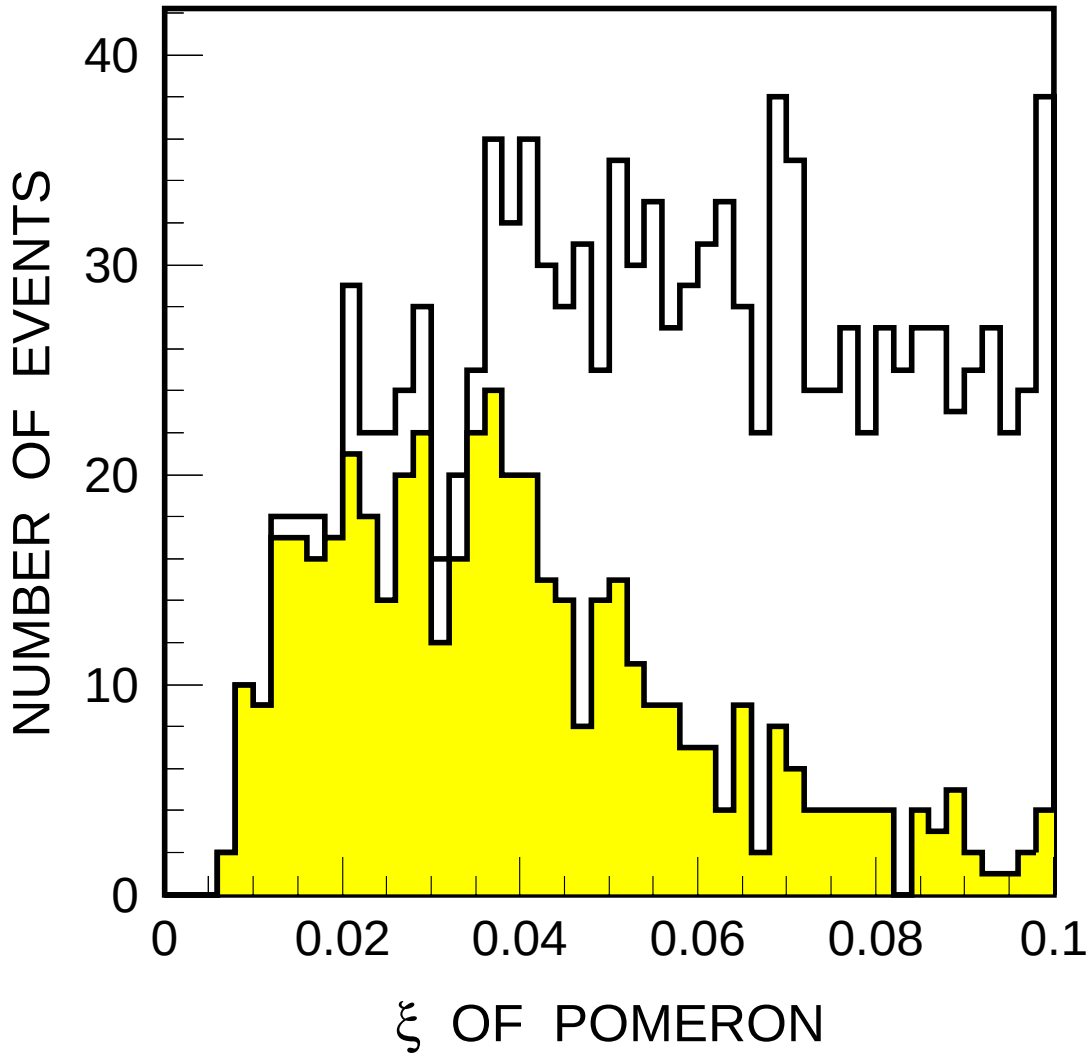

FIG. 3. Monte Carlo distribution of the Pomeron beam momentum fraction, ξ, for diffractive beauty production events with an electron of $9.5 < p_T^e < 20$ GeV/c within $|\eta| < 1.1$, generated using a flat Pomeron structure of gluon to quark ratio $0.7 \div 0.3$. The shaded area is the distributions for events satisfying the rapidity gap requirements.

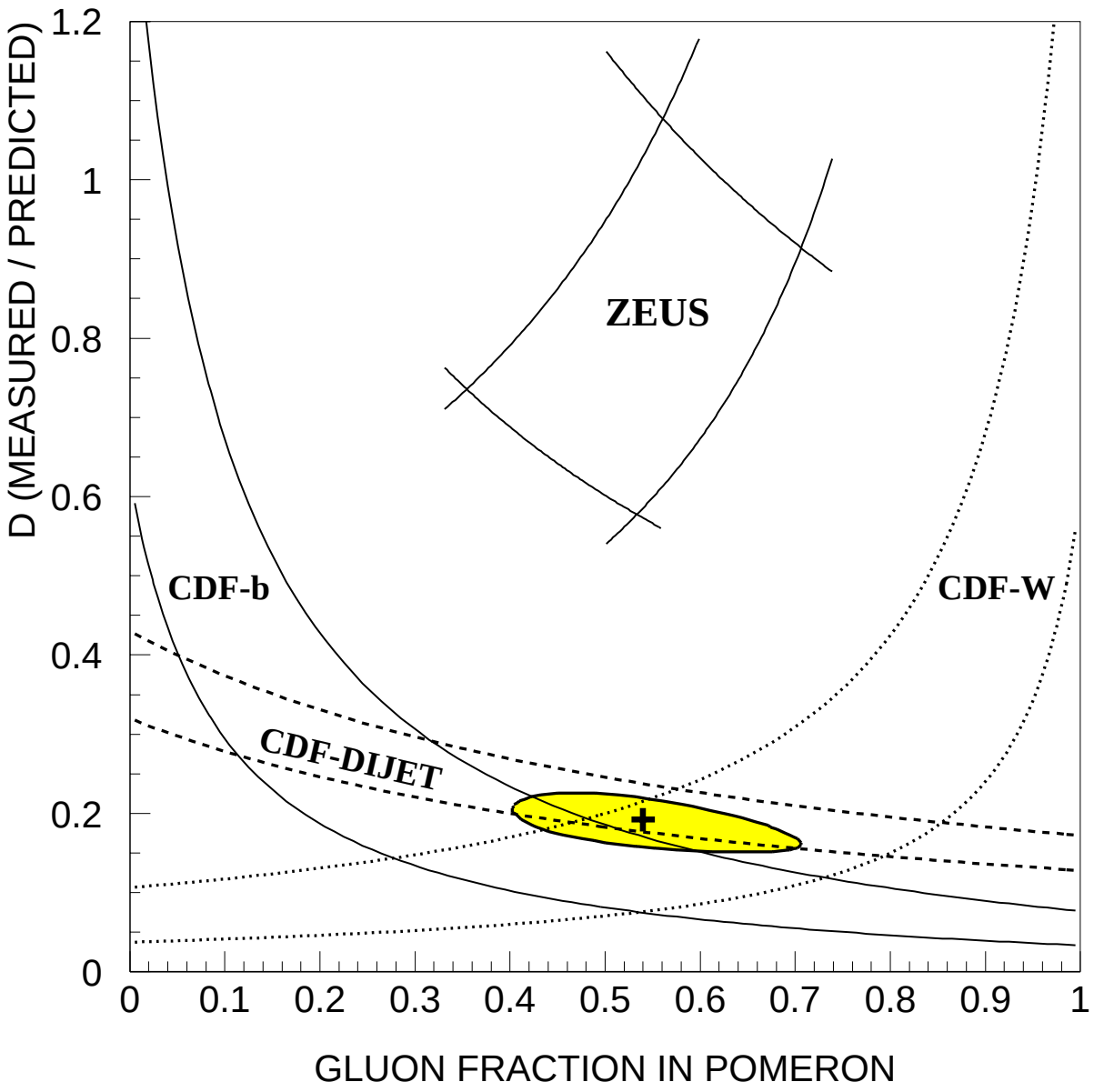

FIG. 4. The ratio, D, of measured to predicted diffractive rates as a function of the gluon content of the Pomeron. The predictions are from POMPYT using the standard Pomeron flux and a hard Pomeron structure. The CDF-W curves were calculated assuming a three-flavor quark structure for the Pomeron. The black cross and shaded ellipse are the best fit and 1σ contour of a least square two-parameter fit to the three CDF results.